# Influence of Donor Configurations on Photophysical, Electrochemical, and Photovoltaic Performances in D−π−A Organic Sensitizers

Qipeng Chai,[§] Wenqin Li,[§] Shiqin Zhu, Qiong Zhang, and Weihong Zhu*

Shanghai Key Laboratory of Functional Materials Chemistry, Key Laboratory for Advanced Materials and Institute of Fine Chemicals, East China University of Science and Technology, Shanghai 200237, P. R. China

ABSTRACT: To optimize light harvesting capabilities, one or two indoline units are introduced as additional donors into the traditional D−π−A model and constructed D−D−π−A sensitizers, **CQ2** and **CQ3**. Absorption spectra and cyclic voltammetry are performed to evaluate the influence of different donor configurations on photophysical and electrochemical properties as well as photovoltaic performances. Incorporating the strong electron-donating indoline unit as an additional donor in **CQ2** and **CQ3** brings several characteristics, such as improving the visible light-harvesting capability and strengthening the intramolecular charge transfer (ICT)

process, as well as positively shifting the HOMO energy level. Moreover, **CQ3** is more dependent upon coadsorbents. Upon coadsorption with 5 mM CDCA, an obvious increment of more than 160% in J_{sc} is achieved for **CQ3**, from 4.26 (without CDCA) to 11.15 mA cm^{-2} (5 mM CDCA). From photovoltaic performances, dye **CQ2** with one additional indoline unit is preferable. Among the three dyes, **CQ2** containing one indoline unit shows the highest conversion efficiency of 6.38%, with the photovoltaic parameters of J_{sc} = 11.33 mA cm^{-2}, V_{oc} = 792 mV, and ff = 0.71 under 100 mW cm^{-2} simulated AM 1.5 G solar irradiation. It is indicative that the incorporation of the additional donor indoline on the framework of the triphenylamine core of **CQ1** is beneficial to the optimization of photovoltaic performances. However, the incorporated multidonor units as additional donors in D-D−π−A type sensitizers can bring deteriorating intermolecular interactions between crowded donor units.

KEYWORDS: Solar cells, Organic sensitizers, Indoline, Donor, Photovoltaic performances
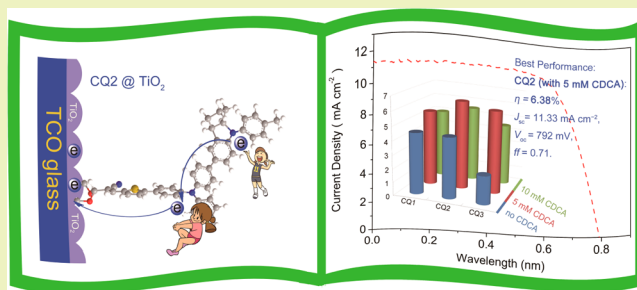
◼ INTRODUCTION

Recently, dye-sensitized solar cells (DSSCs) have attracted considerable attention as an ideal candidate to conventional inorganic photovoltaic devices due to their potentially low cost, easy device fabrication, and relatively high efficiency.[1−5] Although ruthenium (Ru) complexes still stand out as efficient and stable sensitizers, some zinc porphyrin dyes have been proved to show competitive efficiency exceeding 12.0%.[6] Besides, several dipolar metal-free dyes have been reported in recent years, including those based on indoline,[7−10] coumarin,[11,12] triarylamine,[13−18] oligoene,[19] and thiophene[20] dyes.

As light-absorbing materials, dye sensitizers play a vital role in DSSCs. The most popular organic sensitizers are composed of a donor, π-linker, and acceptor moiety (D−π−A) because the configuration can efficiently guarantee the excited electron injection process.[21] Specifically, both the absorption property in the visible region and degree of dye aggregation adsorbed on semiconductor surfaces are vital elements, determining the overall efficiency of organic dyes.[22,23] Triphenylamine is one of the most popular donor moieties due to its powerful electron-donating ability and steric structure.[24−26] Recently, chemical modification of triphenylamine units has been employed to further fine tune the physical and optical properties of sensitizers. Introduction of alkoxy and aromatic groups to

triphenylamine units was reported to tailor energy levels and absorption spectra of sensitizers, resulting in enhanced photocurrent and device efficiency.[27−34] In addition, the nonplanar structure of triphenylamine is beneficial to prevent dye aggregation, which should be avoided in DSSCs because it not only decreases electron injection efficiency but also facilities unfavorable charge recombination between injected electrons and oxidized species near the TiO$_2$ surface.[35]

To date, many structure modifications have been performed on sensitizers to improve their light-harvesting ability and photovoltaic performances.[36,37] For triphenylamine-based dye **CQ1**, the optimizations can be evidently realized by increasing the electron-donating ability of a donor unit via introducing a strong donor (indoline moiety) on the framework of the triphenylamine core to construct so-called D−D−π−A sensitizers, **CQ2** and **CQ3** (Figure 1). As expected, the absorption of **CQ2** and **CQ3** shows significant bathochromic shifts both in solution and adsorption onto the TiO$_2$ electrode. Compared with **CQ1**, the HOMO values for **CQ2** and **CQ3** are shifted positively due to the incorporation of additional
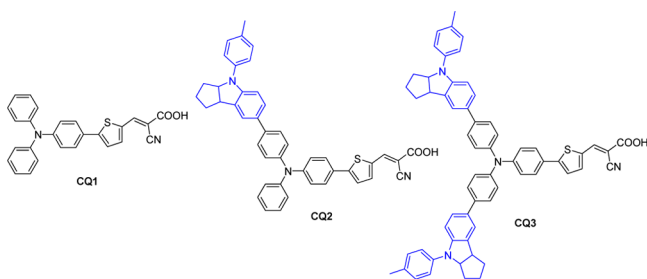
Figure 1. Chemical structures of **CQ1**, **CQ2**, and **CQ3**.

donor units of indoline. However, the relatively low photovoltaic performance of **CQ3** is inconsistent with its excellent light-harvesting abilities and well-matched energy level. We systematically investigated effects of the additional donor number on photovoltaic performances for three dyes.

■ EXPERIMENTAL SECTION

Materials and Characterization. All starting reagents were purchased and purified by the standard method. ^{1}H and ^{13}C NMR spectra were operated at 400 and 100 MHz, respectively, on Bruker AM 400 spectrometer. High resolution mass spectra (HRMS) were obtained with a Waters ESI mass spectrometer. The UV−vis absorption spectra were determined with a CARY 100 spectrophotometer. Cyclic voltammetry was performed by the standard method with a Versastat II electrochemical workstation (Princeton Applied Research).[36]

The fabrication of solar cells with an active area of 0.25 cm[2] as well as photovoltaic measurements were performed according to the published procedures.[36] The redox electrolyte consisted of 0.05 M I$_2$, 0.10 M LiI, 0.60 M PMII, and 0.50 M 4-TBP in a cosolvent of acetonitrile and methoxypropionitrile (volume ratio, 7:3) mixture solution.

Synthesis of 4-Bromo-N-(4-bromophenyl)-N-phenylaniline (2). N-bromosuccinimide (NBS, 2.90 g, 16.30 mmol) was added in portions to a solution of triphenylamine (2.0 g, 8.15 mmol) in CH$_2$Cl$_2$ (25 mL) and stirred for 3 h at room temperature. The reaction mixture was poured into water and extracted with CH$_2$Cl$_2$ (150 mL × 3). The organic layer was combined, and the solvent was removed by rotary evaporation. The residue was used for the next step without any further purification.

Synthesis of 5-(4-((4-Bromophenyl)amino)phenyl)-thiophene-2-carbaldehyde (3). A stirred mixture of compound **2** (1.0 g, 2.48 mmol), Pd(PPh$_3$)$_4$ (40 mg, 0.03 mmol), and K$_2$CO$_3$ (2 M, 10 mL) was dissolved in THF (30 mL), and the mixture was heated to reflux under an argon atmosphere for 30 min. A solution of 5-formyl-2-thiophene-boronic acid (387 mg, 2.48 mmol) in THF (5 mL) was added slowly, and the mixture was further refluxed for 8 h. After cooling to room temperature, the mixture was extracted with CH$_2$Cl$_2$ (50 mL × 3). The organic layer was collected and dried over anhydrous Na$_2$SO$_4$. After the solvent was evaporated, the residue was purified by column chromatography on silica (CH$_2$Cl$_2$: petroleum ether = 1:2) to give a yellow solid (240 mg, Yield 22.3%). ^{1}H NMR (400 MHz, DMSO-d_6, ppm): δ 9.87 (s, 1H), 8.02 (d, J = 4.0 Hz, 1H), 7.72 (d, J = 8.8 Hz, 2H), 7.64 (d, J = 4.0 Hz, 1H), 7.50 (d, J = 8.8 Hz, 2H), 7.36−7.40 (m, 2H), 7.10−7.18 (m, 3H), 7.00−7.02 (m, 4H). ^{13}C NMR (100 MHz, DMSO-d_6, ppm): δ 183.73, 152.64, 148.00, 146.02, 145.88, 141.05, 139.41, 132.45, 129.89, 127.50, 126.05, 125.19, 124.50, 124.21, 122.47, 115.31. HRMS (ESI, m/z): [M + H]$^+$ calcd for C$_{23}$H$_{17}$BrNOS: 434.0214. Found: 434.0219.

Synthesis of 5-(4-(Phenyl(4-(4-(p-tolyl)-1,2,3a,4,8b-hexahydrocyclopenta[b]indol-7-yl)phenyl)amino)phenyl) thiophene-2-carbaldehyde (4). A solution of n-butyllithium (2.5 M in hexane, 1.68 mL, 4.20 mmol) was added dropwise to a solution of bromo-substituted indoline (1.16 g, 3.53 mmol) in THF (25 mL) at −78 °C under an argon atmosphere, and B(OCH$_3$)$_3$ (0.6 mL, 5.30 mmol) was added after the mixture was stirred at −78 °C for 1 h. The

reaction mixture was allowed to warm to room temperature 2 h later and stirred overnight. Without further purification, the mixture was used directly for Suzuki cross-coupling.
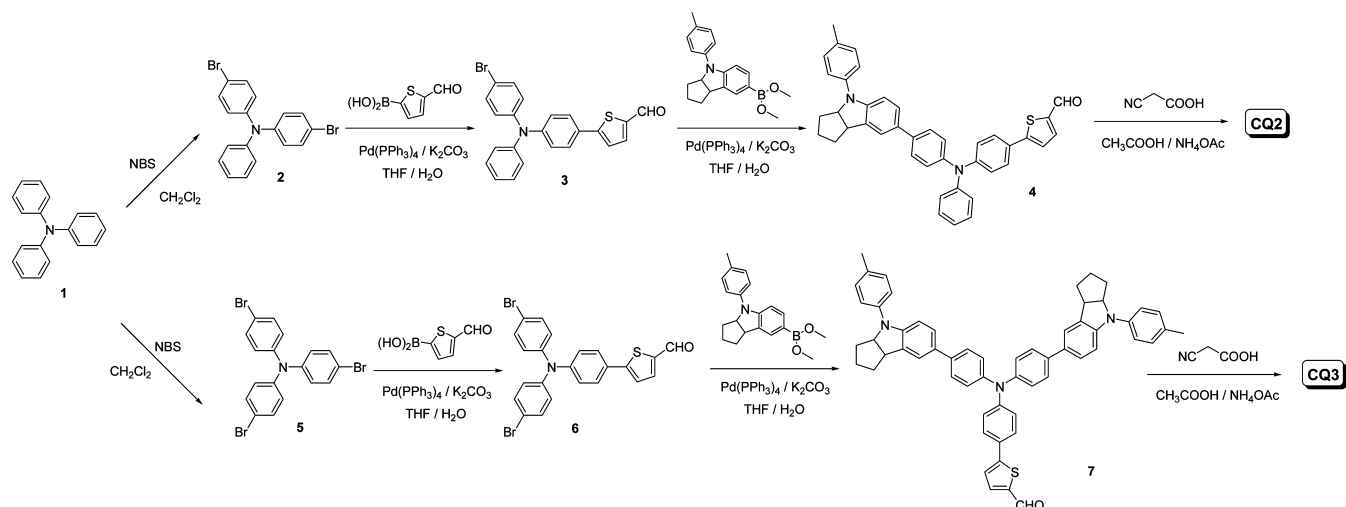
A mixture of 5-(4-((4-bromophenyl)amino)phenyl)thiophene-2-carbaldehyde (240 mg, 0.55 mmol), K$_2$CO$_3$ (2 M, 10 mL), and Pd(PPh$_3$)$_4$ (40 mg, 0.03 mmol) was dissolved in THF (30 mL), and the mixture was heated to reflux under an argon atmosphere for 30 min. Borate ester synthesized previously was added slowly and refluxed for a further 8 h. After cooling to room temperature, the mixture was extracted with CH$_2$Cl$_2$ (50 mL × 3). The organic layer was collected and dried over anhydrous Na$_2$SO$_4$. After the solvent was evaporated, the residue was purified by column chromatography on silica (CH$_2$Cl$_2$: petroleum ether = 1:2) to give an orange solid (120 mg, Yield 36.0%). ^{1}H NMR (400 MHz, DMSO-d_6, ppm): δ 9.87 (s, 1H), 8.01 (d, J = 4.0 Hz, 1H), 7.71 (d, J = 8.8 Hz, 2H), 7.62 (d, J = 4.0 Hz, 1H), 7.58 (d, J = 8.4 Hz, 2H), 7.43 (s, 1H), 7.36−7.39 (m, 2H), 7.32 (d, J = 8.4 Hz, 1H), 7.10−7.22 (m, 9H), 7.01 (d, J = 8.8 Hz, 2H), 6.91 (d, J = 8.4 Hz, 1H). ^{13}C NMR (100 MHz, DMSO-d_6, ppm): δ 183.65, 152.93, 148.50, 146.54, 146.35, 144.39, 140.81, 139.89, 139.45, 136.30, 135.45, 130.30, 129.75, 129.70, 129.57, 127.40, 126.81, 125.41, 125.30, 124.90, 124.04, 123.92, 122.64, 121.63, 119.14, 107.29, 68.17, 44.68, 34.70, 33.24, 24.00, 20.34. HRMS (ESI, m/z): [M + H]$^+$ calcd for C$_{41}$H$_{35}$N$_2$OS: 603.2470. Found: 603.2471.

Synthesis of 2-Cyano-3-(5-(4-(phenyl(4-(4-(p-tolyl)-1,2,3a,4,8b-hexahydrocyclopenta[b]indol-7-yl)phenyl)amino)phenyl)thiophen-2-yl)acrylic Acid (CQ2). Compound **4** (100 mg, 0.17 mmol), cyanoacetic acid (87 mg, 1.02 mmol), ammonium acetate (30 mg, 0.39 mmol), and glacial acetic acid (10 mL) were mixed together and then refluxed for 8 h under an argon atmosphere. The reaction mixture was poured into water and extracted with CH$_2$Cl$_2$. The solvent was removed by rotary evaporation. The residue was purified by column chromatography on silica (CH$_2$Cl$_2$: MeOH = 10:1) to give a red solid (60 mg, Yield 54%). ^{1}H NMR (400 MHz, DMSO-d_6, ppm): δ 8.09 (s, 1H), 7.69 (d, J = 4.0 Hz, 1H), 7.63 (d, J = 8.8 Hz, 2H), 7.57 (d, J = 8.4 Hz, 2H), 7.51 (d, J = 4.0 Hz, 1H), 7.42 (s, 1H), 7.34−7.38 (m, 2H), 7.31 (d, J = 8.4 Hz, 1H), 7.16−7.22 (m, 4H), 7.08−7.12 (m, 5H), 7.02 (d, J = 8.8 Hz, 2H), 6.91 (d, J = 8.4 Hz, 1H), 4.83−4.87 (m, 1H), 3.83−3.87 (m, 1H), 2.28 (s, 3H), 2.02−2.06 (m, 1H), 1.76−1.84 (m, 3H), 1.61−1.64 (m, 1H), 1.37−1.41 (m, 1H). ^{13}C NMR (100 MHz DMSO-d_6, ppm): δ 163.94, 157.08, 148.84, 147.80, 146.49, 146.47, 144.54, 141.07, 139.88, 136.62, 136.01, 135.44, 135.06, 130.24, 129.69, 129.59, 126.96, 126.74, 126.14, 125.35, 125.01, 124.61, 123.77, 123.39, 122.59, 122.19, 119.07, 107.69, 107.29, 68.13, 44.66, 34.70, 33.23, 23.99, 20.33. HRMS (ESI, m/z): [M + H]$^+$ calcd for C$_{44}$H$_{36}$N$_3$O$_2$S: 670.2528. Found: 670.2531.

Synthesis of Tri(4-bromophenyl)amine (5). N-bromosuccinimide (4.64 g, 26.07 mmol) was added in portions to a solution of triphenylamine (2.0 g, 8.15 mmol) in CH$_2$Cl$_2$ (25 mL) at room temperature and stirred for 3 h at room temperature. The reaction mixture was poured into water and extracted with CH$_2$Cl$_2$ (150 mL × 3). The organic layer was dried over anhydrous Na$_2$SO$_4$. After the solvent was evaporated, the crude product was purified by recrystallization from ethanol to afford a white solid (3.54 g, Yield 90%).

Synthesis of 5-(4-(Bis(4-bromophenyl)amino)phenyl)-thiophene-2-carbaldehyde (6). A stirred mixture of compound **5** (1.0 g, 2.07 mmol), Pd(PPh$_3$)$_4$ (40 mg,0.03 mmol), and a K$_2$CO$_3$ solution (2 M, 10 mL) was dissolved in THF (30 mL) and heated to reflux under an argon atmosphere for 30 min. A solution of 5-formyl-2-thiophene-boronic acid (323 mg, 2.07 mmol) in THF (5 mL) was added slowly, and the mixture was refluxed for another 8 h. After cooling to room temperature, the mixture was extracted with CH$_2$Cl$_2$ (50 mL × 3). The organic layer was collected and dried over anhydrous Na$_2$SO$_4$. After the solvent was evaporated, the residue was purified by column chromatography on silica (CH$_2$Cl$_2$: petroleum ether = 1:2) to give a yellow solid (246 mg, Yield 23.1%). ^{1}H NMR (400 MHz, DMSO-d_6, ppm): δ 9.88 (s, 1H), 8.02 (d, J = 4.0 Hz, 1H), 7.74 (d, J = 8.8 Hz, 2H), 7.65 (d, J = 4.0 Hz, 1H), 7.52 (d, J = 8.8 Hz, 4H), 7.02−7.06 (m, 6H). ^{13}C NMR (100 MHz, DMSO-d_6, ppm): δ 183.80, 152.43, 147.53, 145.51, 141.23, 139.41, 132.61, 127.61, 126.86,

Scheme 1. Synthetic Routes of CQ2 and CQ3

126.42, 124.44, 123.13, 115.86. HRMS (ESI, *m/z*): [M + H]⁺ calcd for C₂₃H₁₆NOSBr₂: 511.9319. Found: 511.9323.

Synthesis of 5-(4-(Bis(4-(4-(p-tolyl)-1,2,3a,4,8b-hexahydrocyclopenta[b]indol-7-yl)phenyl)amino)phenyl) thiophene-2-carbaldehyde (7). A mixture of compound **6** (240 mg, 0.47 mmol), K₂CO₃ (2 M, 10 mL), and Pd(PPh₃)₄ (40 mg, 0.03 mmol) was dissolved in THF (30 mL) and heated to reflux under an argon atmosphere for 30 min. Borate ester synthesized previously was added slowly and refluxed for a further 8 h. After cooling to room temperature, the mixture was extracted with CH₂Cl₂ (50 mL × 3). The organic layer was collected and dried over anhydrous Na₂SO₄. After the solvent was evaporated, the residue was purified by column chromatography on silica (CH₂Cl₂: petroleum ether = 1:2) to give an orange solid (150 mg, Yield 37.7%). ¹H NMR (400 MHz, DMSO-*d₆*, ppm): δ 9.87 (s, 1H), 8.01 (d, *J* = 4.0 Hz, 1H), 7.71 (d, *J* = 8.8 Hz, 2H), 7.62 (d, *J* = 4.0 Hz, 1H), 7.58 (d, *J* = 8.8 Hz, 4H), 7.43 (s, 2H), 7.31 (d, *J* = 8.36 Hz, 2H), 7.12−7.21 (m, 12H), 7.03 (d, *J* = 8.8 Hz, 2H), 6.91 (d, *J* = 4.0 Hz, 1H), 4.82−4.87 (m, 2H), 3.83−3.86 (m, 2H), 2.28 (s, 6H), 2.01−2.06 (m, 2H), 1.75−1.84 (m, 6H), 1.59−1.64 (m, 2H), 1.37−1.41 (m, 2H). ¹³C NMR (100 MHz, DMSO-*d₆*, ppm): δ 183.63, 152.96, 148.41, 146.49, 144.32, 140.74, 139.86, 139.48, 136.20, 135.45, 130.25, 129.69, 129.56, 127.37, 126.78, 125.38, 125.21, 123.87, 122.61, 121.60, 119.07, 107.28, 68.13, 44.66, 34.71, 33.23, 24.00, 20.33. HRMS (ESI, *m/z*): [M + H]⁺ calcd for C₅₉H₅₂N₃OS: 850.3831. Found: 850.3832.

Synthesis of 3-(5-(4-(Bis(4-(4-(p-tolyl)-1,2,3a,4,8b-hexahydrocyclopenta[b]indol-7-yl)phenyl)amino)phenyl) thiophene-2-yl)-2-cyanoacrylic Acid (CQ3). Compound **7** (120 mg, 0.14 mmol), cyanoacetic acid (71 mg, 0.83 mmol), ammonium acetate (30 mg, 0.39 mmol), and glacial acetic acid (10 mL) were mixed together and then refluxed for 8 h under an argon atmosphere. The mixture was washed with water three times and extracted with CH₂Cl₂ (50 mL × 3). The solvent was removed by rotary evaporation. The residue was purified by column chromatography on silica (CH₂Cl₂: MeOH = 10:1) to give a red solid (70 mg, Yield 54%). ¹H NMR (400 MHz, DMSO-*d₆*, ppm): δ 8.11 (s, 1H), 7.72 (d, *J* = 4.0 Hz, 1H), 7.64 (d, *J* = 8.8 Hz, 2H), 7.57 (d, *J* = 8.4 Hz, 4H), 7.53 (d, *J* = 3.6 Hz, 1H), 7.43 (s, 2H), 7.31 (d, *J* = 8.4 Hz, 2H), 7.11−7.21 (m, 12H), 7.05 (d, *J* = 8.4 Hz, 2H), 6.91 (d, *J* = 8.0 Hz, 2H), 4.83−4.86 (m, 2H), 3.82−3.86 (m, 2H), 2.28 (s, 6H), 1.99−2.04 (m, 2H), 1.75−1.84 (m, 6H), 1.60−1.63 (m, 2H), 1.38−139 (m, 2H). ¹³C NMR (100 MHz, DMSO-*d₆*, ppm): δ 163.78, 148.07, 146.47, 144.38, 139.86, 136.08, 135.45, 134.35, 130.24, 129.69, 129.57, 127.15, 126.75, 125.68, 125.36, 125.09, 123.57, 122.58, 121.93, 119.06, 118.08, 107.29, 68.12, 44.65, 34.70, 33.22, 23.99, 20.32. HRMS (ESI, *m/z*): [M + H]⁺ calcd for C₆₂H₅₃N₄O₂S: 917.3889. Found: 917.3894.

■ RESULTS AND DISCUSSION

Design and Synthesis. For increasing the donor capability and optimizing the light-harvesting and energy levels, either one or two indoline moieties were incorporated into the triphenylamine unit as an additional donor to develop two D−D−π−A dyes, **CQ2** and **CQ3** (Figure 1). Their synthetic routes are illustrated in Scheme 1, with commercially available starting materials. Bromination of triphenylamine was carried out with either two or three equivalent NBS to yield **2** and **5**, respectively. 5-Formyl-2-thiopheneboronic acid is attached to the core triphenylamine by the Suzuki coupling reaction to obtain two important intermediates, **3** and **6**. Further Suzuki coupling reactions introduced mono- or di-functionalized indoline groups to afford the aldehydes of **4** and **7**. The two targeted dyes were obtained by condensation of the corresponding aldehydes with cyanoacetic acid via the Knoevenagel reaction in the presence of acetic acid and ammonium acetate.

Photophysical and Electrochemical Properties. Figure 2 presents the UV−vis absorption spectra of three dyes (**CQ1−CQ3**) in chloroform and on TiO₂ film, and the corresponding data are summarized in Table 1. In the visible range, **CQ1**, **CQ2**, and **CQ3** show typical and strong absorption bands located at 442, 458, and 479 nm, respectively, which arise from the intramolecular charge transfer (ICT) from the donor to the acceptor moiety.[38] With respect to the reference dye **CQ1**, the absorption peaks for **CQ2** and **CQ3** were red-shifted by 16 and 37 nm, along with 45% and 59% enhancement in their molar extinction coefficients, respectively. In the UV region, the absorption around 300−400 nm that originated from a π−π* transition for **CQ2** and **CQ3** was significantly larger than that for **CQ1**. Obviously, compared with the reference dye of **CQ1**, such a bathochromic shift with higher absorption coefficients in **CQ2** and **CQ3** can be ascribed to the incorporation of the additional powerful electron-donating moieties of indoline.[39]

Figure 2b depicts the absorption spectra of **CQ1**, **CQ2**, and **CQ3** on 3 μm thin TiO₂ films after 0.5 h adsorption. The maximal absorption peaks for **CQ1**, **CQ2**, and **CQ3** on 3 μm TiO₂ films were located at 429, 440, and 465 nm, respectively, and blue-shifted by 13, 18, and 14 nm, respectively, with respect to CHCl₃. Generally, when anchored onto a nanocrystalline TiO₂ surface, the deprotonation and aggregation of dye molecules have an effect on absorption profiles. Deprotonation
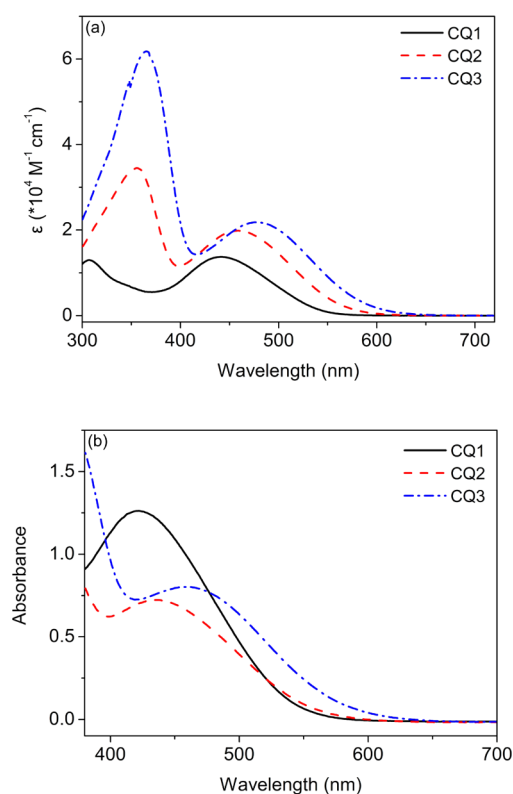
Figure 3. Cyclic voltammograms of sensitizers **CQ1**, **CQ2**, and **CQ3** in CH$_3$CN containing 0.1 M TBAPF$_6$ as supporting electrolyte.

Figure 2. UV−vis absorption spectra of sensitizers **CQ1**, **CQ2**, and **CQ3** measured in CHCl$_3$ (a) and adsorbed on 3 μm TiO$_2$ films (b).

Table 1. Photophysical and Electrochemical Properties of Sensitizers CQ1, CQ2, and CQ3 in CHCl$_3$ and on TiO$_2$ Films

dyes	CQ1	CQ2	CQ3
$\lambda_{max}{}^a$ (nm)	442 (13700)	458 (19800)	479 (21800)
ε^a (M^{-1} cm^{-1})	307 (13000)	356 (34500)	365 (61800)
λ_{max} on TiO$_2{}^b$ (nm)	429	440	465
HOMO^c (V)	1.16	0.76	0.74
$E_{0-0}{}^d$ (eV)	2.27	2.12	2.06
LUMO^d (V)	−1.11	−1.36	−1.32

^{a}Absorption peaks (λ_{max}) and molar extinction coefficients (ε) in CHCl$_3$ solution. ^{b}Absorption peaks on 3 μm TiO$_2$ films. ^{c}HOMO was measured in acetonitrile solution, calibrated with ferrocene/ferrocenium (Fc/Fc$^+$) as an external reference. ^{d}E$_{0-0}$ was estimated from the absorption thresholds from absorption spectra of dyes adsorbed on the TiO$_2$ film. LUMO is estimated by subtracting E_{0-0} from the HOMO.

and *H*-aggregates always result in the blue-shift of an absorption band, while *J*-aggregates mainly lead to a red-shift.[40] Here, the observed blue-shift absorption may possibly result from the deprotonation of cyanoacetic carboxylic acid or *H*-aggregates.

Electrochemical Properties. Energy levels of sensitizers are crucial to judge the possibilities of electron injection and dye regeneration in DSSCs devices. Cyclic voltammogram (CV) was performed with three sensitizers in CH$_3$CN containing 0.1 M TBAPF$_6$ as the supporting electrolyte (Figure 3). The HOMO and LUMO levels of these dyes were summarized in Table 1. The first oxidation potentials of the three dyes (1.16, 0.76, and 0.74 V for **CQ1**, **CQ2**, and **CQ3**, respectively), corresponding to HOMO values, are more positive than that of I$_3^-$/I$^-$, ensuring the thermodynamic
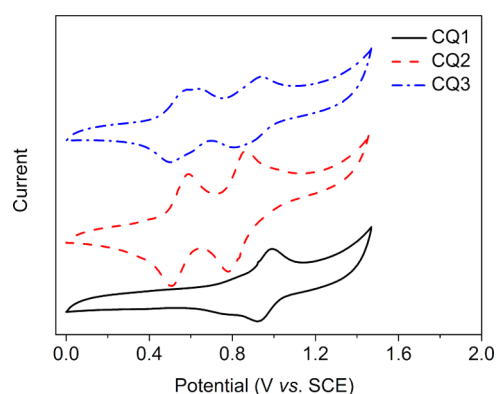
regeneration of dyes.[41] As estimated from the absorption threshold of these dyes onto TiO$_2$ films, the resulting E_{0-0} is 2.27, 2.12, and 2.06 eV for **CQ1**, **CQ2**, and **CQ3** (Table 1), respectively. Consequently, all the LUMO values of these dyes (−1.11, −1.36, and −1.32 V, respectively) are more negative than the conduction band edge of TiO$_2$, indicating a sufficient driving force for electron injection from the excited dye molecules to the conduction band of TiO$_2$.[42] Notably, with respect to **CQ1**, the incorporation of an indoline unit in **CQ2** and **CQ3** as an additional donor does have an obvious effect on the HOMO orbital and shifts the oxidation potential (HOMO) cathodically by more than 0.40 V, which is ascribed to the beneficial charge transfer process upon the contribution from the indoline auxiliary donor. That is, it is easier to generate a photon electron for D−D−π−A sensitizers such as **CQ2** and **CQ3**.

Theory Approach. The electronic configurations were further calculated by theoretical models implanted in the Gaussian 09 package.[43] Their molecular geometries were optimized using the hybrid B3LYP functional and the standard 6-31G(d) basis set.[44] For the TD-DFT calculations, performed on the B3LYP optimized ground-state geometries, the Coulomb attenuating B3LYP (CAM-B3LYP) approach was used with the 6-31+G(d) basis set.[45] The solvation effect was taken into account in the TD-DFT calculations in CHCl$_3$ with the nonequilibrium version of the C-PCM model implemented in Gaussian09.[43] According to the optimized molecular geometry in Figure 4, the incorporation of an indoline unit has a negligible effect on the conformation of two adjacent phenyl groups within triphenylamine, and the variation of the calculated value for the dihedral angle between benzene and thiophene rings is less than 3°. Besides, the orientation of the two adjacent phenyl rings of indoline and triphenylamine is fundamentally equal for **CQ2** and **CQ3**.

TD-DFT calculated eigenvectors in Table 2 provide theoretical absorption spectra of these dyes, in good accordance with the experimental optical properties. As shown in Figure 5, the HOMO and HOMO−1 orbital for **CQ1** is mainly delocalized over the whole structure, whereas the electron density of LUMO is mainly populated on the conjugated bridge and acceptor unit. Obviously, there is good overlap between the former and the latter. The absorption bands for **CQ1** are mainly ascribed to the electronic transitions of HOMO→ LUMO and HOMO−1 → LUMO with contribution of 81% and 69%, respectively. Accordingly, the two charge transfer
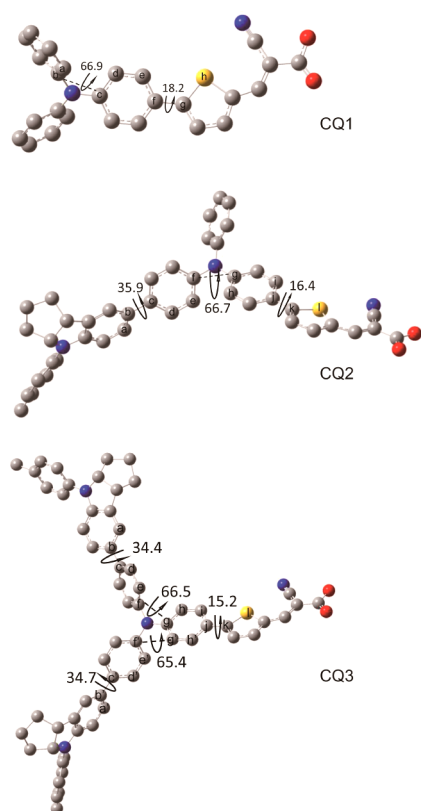
Figure 4. Optimized ground-state geometries for sensitizers **CQ1**, **CQ2**, and **CQ3**.

Table 2. Calculated TDDFT (CAMB3LYP) Excitation Energies for the Lowest Transition (eV, nm), Oscillator Strengths (*f*), Composition in Terms of Molecular Orbital Contributions, and Experimental Absorption Maxima for Sensitizers CQ1, CQ2, and CQ3

dyes	state	composition[a]	E (eV, nm)	f	exp. (eV, nm)
CQ1	S1	81% H→ L	2.79 (444)	1.2718	2.80 (442)
	S2	69% H−1 → L	3.87 (320)	0.1172	4.04 (307)
CQ2	S1	34% H→ L	2.72 (455)	1.4096	2.71 (458)
		49% H−1→ L			
	S2	49% H→ L	3.58 (346)	0.0683	3.48 (356)
		24% H−2 → L			
CQ3	S1	48% H→ L	2.66 (466)	1.414	2.58 (479)
		37% H−2 → L			
	S2	40% H→ L	3.52 (352)	0.1156	3.40 (365)
		30% H−3 → L			

[a]H = HOMO, L = LUMO, H−1 = HOMO−1, H−2 = HOMO−2, H−3 = HOMO−3.

processes originated by light harvesting are beneficial to the charge transfer process.

The electronic transitions for **CQ2** and **CQ3** become more complicated. Taking **CQ2** for example, the HOMO orbital is mainly located at the donor part, and the HOMO−1 and HOMO−2 orbitals are delocalized over the whole structure. Especially, the electron contribution from the additional donor of an indoline unit decreases in the order of HOMO > HOMO−1 > HOMO−2. The LUMO orbital is a π orbital crossing the conjunction and acceptor. According to the TD-DFT calculation, the absorption band of **CQ2** is attributed to HOMO→LUMO, HOMO−1→LUMO, and HOMO−2→
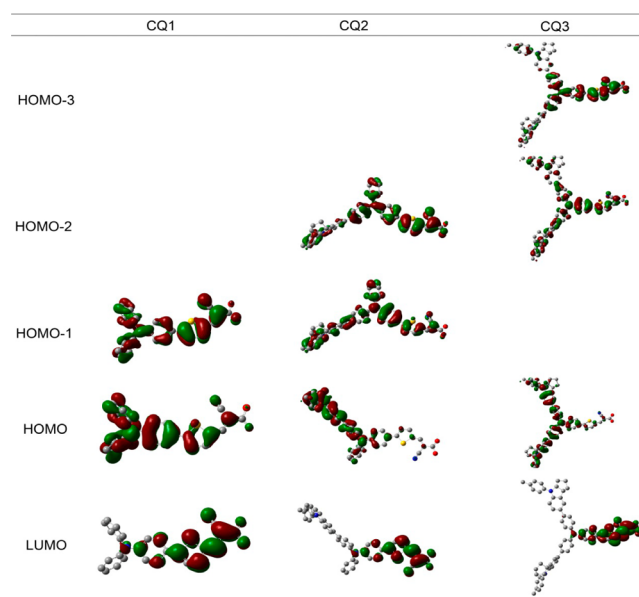

Figure 5. Calculated frontier orbitals of sensitizers **CQ1**, **CQ2**, and **CQ3** (iso-density = 0.020 au).

LUMO. All three electronic transitions correspond to an electron transfer from the whole molecule to the anchoring group, which is beneficial to the electron injection process.

Photovoltaic Performances. The action spectra of monochromatic incident photon-to-electron conversion efficiency (IPCE) for DSSCs based on **CQ1**, **CQ2**, and **CQ3** coadsorbed with 5 mM CDCA was measured with the wavelength of 300−800 nm. As shown in Figure 6a, the IPCE onsets for **CQ1**, **CQ2**, and **CQ3** are 650, 710, and 740 nm, respectively, along with an increase in the order of **CQ1** < **CQ2** < **CQ3**. This is in good agreement with their absorption spectra on TiO$_2$ films. The solar cells based on **CQ1** show high IPCEs above 70% in the range of 410−460 nm and decrease sharply at 500−600 nm with a narrow profile. While for **CQ2** and **CQ3**, their IPCE plateaus are located at 410−500 nm and 440−530 nm, with a broader profile than that of **CQ1**. Accordingly, the incorporation of an indoline group as an additional donor can efficiently extend the IPCE onset of **CQ2** and **CQ3**, which is highly beneficial to harvest the light photons in the visible region as well as even in part of the NIR region.

Figure 6b presents the I−V curves of the cells measured under simulated 1.5 air mass global solar light conditions (100 mW cm^{-2}), and the detailed parameters were collected in Table 3. Coadsorbent CDCA was introduced into the dye bath for breaking up the dye aggregation when coated onto TiO$_2$ films.[39] As shown in Table 3, the highest power conversion efficiency for three dyes was obtained when competitively adsorbed with 5 mM CDCA. The photocurrent destiny for **CQ2** and **CQ3** was 11.33 and 11.15 mA cm^{-2}, almost 15% higher than **CQ1**, ascribed to the relatively broader absorption profile. In contrast, there was no obvious enhancement of V_{oc} in **CQ2** and **CQ3**. Under optimized conditions, among the three dyes, **CQ2** achieved the highest conversion efficiency of 6.38% with the parameters of J_{sc} = 11.33 mA cm^{-2}, V_{oc} = 792 mV, and *ff* = 0.71 (Table 3).

To further optimize the dye adsorption process, a different co-adsorption concentration of CDCA was used as coadsorbents with sensitizers when the TiO$_2$ films were dipped into the chloroform solutions (Table 3). As demonstrated, the
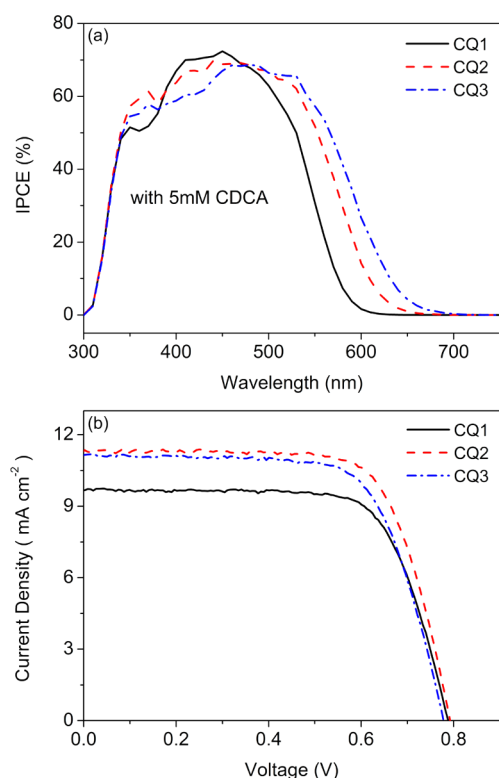
Figure 6. IPCE action spectra (a) and photocurrent−voltage characteristics (b) of DSSCs based on sensitizers **CQ1**, **CQ2**, and **CQ3** coadsorbed with 5 mM CDCA.

Table 3. Effect of CDCA on Photovoltaic Performances of Sensitizers CQ1, CQ2, and CQ3

dyes	CDCA (mM)	amount (10^{-8} mol cm^{-2})	J_{sc} (mA cm^{-2})	V_{oc} (mV)	ff	η (%)
CQ1	0	7.36	8.73	761	0.68	4.50
	5	5.15	9.72	787	0.71	5.45
	10	4.43	9.86	767	0.66	4.99
CQ2	0	6.65	8.91	753	0.66	4.44
	5	4.26	11.33	792	0.71	6.38
	10	3.58	9.82	770	0.73	5.49
CQ3	0	6.12	4.26	739	0.66	2.08
	5	3.98	11.15	778	0.69	5.99
	10	3.32	8.94	781	0.64	4.47

absorption intensity of **CQ1**, **CQ2**, and **CQ3** become decreased gradually along with the increasing concentration of CDCA, indicative of the coexistence of competitive adsorption between dye molecules and coadsorbent CDCA. Impressively, when the concentration of CDCA varied from 0 to 5 mM, the absorbance of the three dyes decreases significantly by 30−40%. However, there is no distinct absorption change with further increments from 5 to 10 mM. That is, the aggregation can be effectively suppressed with assistance of 5 mM CDCA.

Figure 7 shows the IPCE of three dyes with different coadsorption concentrations of CDCA. With increasing the content of CDCA from 0 to 5 mM, the three dye-based cells show a notable difference. For **CQ1**, there is only a tiny increment on the height of IPCE, while for **CQ2** there is a 20% improvement for the wavelengths of 450−530 nm. The most prominent increment for **CQ3** arises from 30% to 70%. Here, the change in the height of IPCE results from the different
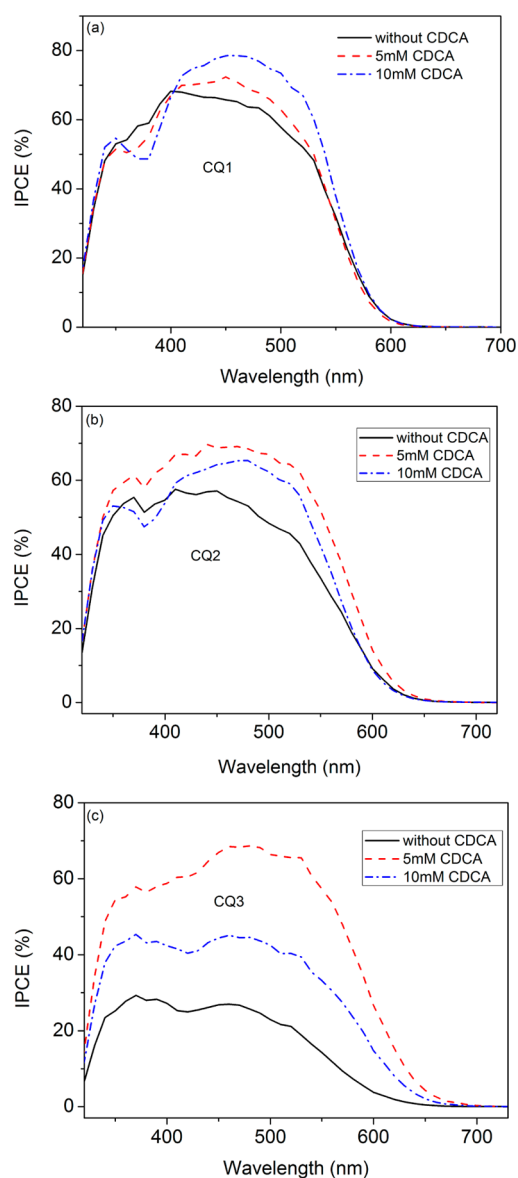

Figure 7. Different CDCA concentration dependencies of IPCE of **CQ1**, **CQ2**, and **CQ3**.

electron injection efficiency. Obviously, the distinct difference among the three sensitizers coadsorbed with 5 mM CDCA can disclose the different degrees of intermolecular interactions to some extent.

Impressively, without coadsorption, the J_{sc} of **CQ3** (4.26 mA cm^{-2}) is much lower than that of **CQ2** (8.91 mA cm^{-2}) and **CQ1**. Along with the introduction of 5 mM of CDCA as coadsorbent, an obvious increment of more than 160% in J_{sc} was achieved for **CQ3**, from 4.26 (without CDCA) to 11.15 mA cm^{-2} (5 mM CDCA). Generally, the photocurrent is determined by the light-harvesting ability of the sensitizer, dye absorption amount, and electron injection efficiency.[1,46] Considering that the absorption property and energy level for **CQ3** is perfectly acceptable, we shed light on the intermolecular interaction with the adsorption amounts (Table 3). The adsorbed amount for **CQ3** without CDCA was 6.12×10^{-8} mol cm^{-2}, which is comparable to that of **CQ2** (6.65×10^{-8} mol cm^{-2}). That means, in **CQ2** and **CQ3**, that the donor part with one or two indoline units does not have
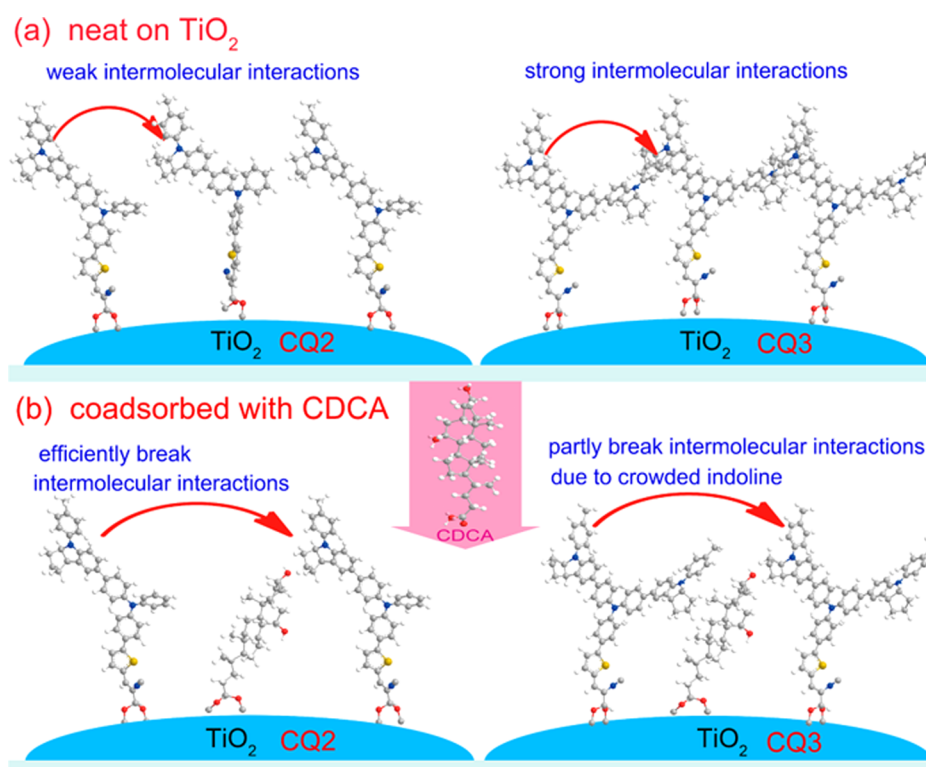
244

dx.doi.org/10.1021/sc400293v | ACS Sustainable Chem. Eng. 2014, 2, 239−247

Figure 8. Schematic diagram of sensitizers **CQ2** and **CQ3** adsorbed on a TiO$_2$ surface without (top) and with (bottom) 5 mM CDCA.

much of an effect on the adsorption amounts.[33,39] When coadsorbed with 5 mM CDCA, their adsorption amounts onto TiO$_2$ were decreased by nearly 35−40%. Figure 8 shows the possible mechanisms of the CDCA effect on dye adsorption on the TiO$_2$ surface and the photovoltaic properties. With almost the same adsorption amount, **CQ2**, containing one indoline as an additional donor, can adsorb onto the TiO$_2$ film in an ordered manner to some extent. That is, the donor moieties tend to offset one another in adjacent horizon, and the intermolecular interactions (such as intermolecular energy transfer or electron transfer) may be prevented efficiently (Figure 8a). In contrast, when **CQ3** is adsorbed onto a TiO$_2$ surface without CDCA, the two incorporated indoline units as additional donors might be too near the other molecules, along with an increase in the possible interactions between indoline units, which results in the excited-state quenching of the dye with a loss of photocurrent (Figure 8).[47−50] When coadsorbed with CDCA, the dye loading amount was decreased, and the interactions between intermolecular indoline units can be blocked to a degree due to the increased distance of intermolecular indoline units (Figure 8b), thus distinctly improving the photocurrent J_{sc} of **CQ3**. Further improving the content of CDCA, the decreased photocurrent J_{sc} may arise from the less dye-loading amount. While for **CQ2**, the introduction of 5 mM CDCA can block the interactions of the indoline moieties more efficiently, thus leading to a better performance. From the above analysis, upon incorporation from one indoline unit (**CQ2**) to two indoline units (**CQ3**), the photoresponsive wavelength as well as absorption coefficients can be increased. However, from the viewpoint of photovoltaic performances, dye **CQ2** with one additional donor unit is preferable. We should keep in mind that the incorporated multidonor units such as **CQ3** can bring

deteriorating intermolecular interactions between crowded intermolecular donor units (Figure 8b).

CONCLUSIONS

In summary, either one or two indoline moieties have been introduced into the framework of the triphenylamine unit in **CQ1** as an additional donor to construct D−D−π−A sensitizers, **CQ2** and **CQ3**. Their light-harvesting capabilities, energy levels, and photovoltaic performances were well studied. Compared with **CQ1**, the HOMO values for **CQ2** and **CQ3** are shifted positively due to the incorporation of an additional indoline donor. Upon incorporation from one indoline unit (**CQ2**) to two indoline units (**CQ3**), the photoresponsive wavelength as well as absorption coefficients can be increased. As demonstrated, **CQ3** is more dependent upon coadsorbents. Upon coadsorption with 5 mM CDCA, an obvious increment of more than 160% in J_{sc} was achieved for **CQ3** from 4.26 (without CDCA) to 11.15 mA cm^{-2} (5 mM CDCA). From photovoltaic performances, dye **CQ2** with one additional indoline unit is preferable. It is essential to notice that the incorporated multidonor units as additional donors in D-D−π−A type sensitizers can bring deteriorating intermolecular interactions between crowded intermolecular donor units.

AUTHOR INFORMATION

Corresponding Author
*E-mail: whzhu@ecust.edu.cn. Fax: (+86) 21-6425-2758.
Author Contributions
§C.Q.P. and L.W.Q. contributed equally to this work.
Notes
The authors declare no competing financial interest.

■ REFERENCES

(1) O'Regan, B.; Grätzel, M. A low-cost, high-efficiency solar cell based on dye-sensitized colloidal TiO₂ films. *Nature* **1991**, *353*, 737–740.

(2) Cha, S. I.; Kim, Y.; Hwang, K. H.; Shin, Y.-J.; Seo, S. H.; Lee, D. Y. Dye-sensitized solar cells on glass paper: TCO-free highly bendable dye-sensitized solar cells inspired by the traditional Korean door structure. *Energy Environ. Sci.* **2012**, *5*, 6071–6075.

(3) Wu, Y. Z.; Zhu, W. H. Organic sensitizers from D−π−A to D−A−π−A: Effect of the internal electron-withdrawing units on molecular absorption, energy levels and photovoltaic performances. *Chem. Soc. Rev.* **2013**, *42*, 2039–2058.

(4) Ooyama, Y.; Harima, Y. Molecular designs and syntheses of organic dyes for dye-sensitized solar cells. *Eur. J. Org. Chem.* **2009**, 2903–2934.

(5) Wang, L.; Zhang, H.; Wang, C. L.; Ma, T. L. Highly stable gel-state dye-sensitized solar cells based on high soluble polyvinyl acetate. *ACS Sustainable Chem. Eng.* **2013**, *1*, 205–208.

(6) Yella, A.; Lee, H. W.; Tsao, H. N.; Yi, C.; Chandiran, A. K.; Nazeeruddin, M. K.; Diau, E. W.; Yeh, C. Y.; Zakeeruddin, S. M.; Grätzel, M. Porphyrin-sensitized solar cells with cobalt (II/III)−based redox electrolyte exceed 12% efficiency. *Science* **2011**, *334*, 629–634.

(7) Horiuchi, T.; Miura, H.; Sumioka, K.; Uchida, S. High efficiency of dye-sensitized solar cells based on metal-free indoline dyes. *J. Am. Chem. Soc.* **2004**, *126*, 12218–12219.

(8) Horiuchi, T.; Miura, H.; Uchida, S. Highly-efficient metal-free organic dyes for dye-sensitized solar cells. *Chem. Commun.* **2003**, 3036–3037.

(9) Wu, Y. Z.; Zhang, X.; Li, W. Q.; Wang, Z. S.; Tian, H.; Zhu, W. H. Hexylthiophene-featured D−A−π−A structural indoline chromophores for coadsorbent-free and panchromatic dye-sensitized solar cells. *Adv. Energy Mater.* **2012**, *2*, 149–156.

(10) Pei, K.; Wu, Y. Z.; Wu, W. J.; Zhang, Q.; Chen, B. Q.; Tian, H.; Zhu, W. H. Constructing organic D−A−π−A-featured sensitizers with a quinoxaline unit for high-efficiency solar cells: The effect of an auxiliary acceptor on the absorption and the energy level alignment. *Chem.—Eur. J.* **2012**, *18*, 8190–8200.

(11) Wang, Z. S.; Cui, Y.; Hara, K.; Dan-oh, Y.; Kasada, C.; Shinpo, A. A high-light-harvesting-efficiency coumarin dye for stable dye-sensitized solar cells. *Adv. Mater.* **2007**, *19*, 1138–1141.

(12) Hara, K.; Wang, Z. S.; Sato, T.; Furube, A.; Katoh, R.; Sugihara, H.; Dan-oh, Y.; Kasada, C.; Shinpo, A.; Suga, S. Oligothiophene-containing coumarin dyes for efficient dye-sensitized solar cells. *J. Phys. Chem. B* **2005**, *109*, 15476–15482.

(13) Liang, M.; Xu, W.; Cai, F. S.; Chen, P. Q.; Peng, B.; Chen, J.; Li, Z. M. New triphenylamine-based organic dyes for efficient dye-sensitized solar cells. *J. Phys. Chem. C* **2007**, *111*, 4465–4472.

(14) Ko, S.; Choi, H.; Kang, M.-S.; Hwang, H.; Ji, H.; Kim, J.; Ko, J.; Kang, Y. Silole-spaced triarylamine derivatives as highly efficient organic sensitizers in dye-sensitized solar cells. *J. Mater. Chem.* **2010**, *20*, 2391–2399.

(15) Zhang, M.-D.; Pan, H.; Ju, X.-H.; Ji, Y.-J.; Qin, L.; Zheng, H.-G.; Zhou, X.-F. Improvement of dye-sensitized solar cells' performance through introducing suitable heterocyclic groups to triarylamine dyes. *Phys. Chem. Chem. Phys.* **2012**, *14*, 2809–2815.

(16) Liu, J.; Zhou, D.; Wang, F.; Fabregat-Santiago, F.; Miralles, S. G.; Jing, X.; Bisquert, J.; Wang, P. Joint photophysical and electrical analyses on the influence of conjugation order in D−π−A photo-

sensitizers of mesoscopic titania solar cells. *J. Phys. Chem. C* **2011**, *115*, 14425–14430.

(17) Shi, J.; Chen, J.; Chai, Z.; Wang, H.; Tang, R.; Fan, K.; Wu, M.; Han, H.; Qin, J.; Peng, T.; Li, Q.; Li, Z. High performance organic sensitizers based on 11,12-bis(hexyloxy) dibenzo[*a,c*]phenazine for dye-sensitized solar cells. *J. Mater. Chem.* **2012**, *22*, 18830–18838.

(18) Li, Q. Q.; Shi, J.; Li, H. Y.; Li, S.; Zhong, C.; Guo, F. L.; Li, Zhen Novel pyrrole-based dyes for dye-sensitized solar cells: from rod-shape to "H" type. *J. Mater. Chem.* **2012**, *22*, 6689–6696.

(19) Katoh, R.; Furube, A.; Mori, S.; Miyashita, M.; Sunahara, K.; Koumura, N.; Hara, K. Highly stable sensitizer dyes for dye-sensitized solar cells: Role of the oligothiophene moiety. *Energy Environ. Sci.* **2009**, *2*, 542–546.

(20) Ren, X.; Jiang, S.; Cha, M.; Zhou, G.; Wang, Z. S. Thiophene-bridged double D−π−A dye for efficient dye-sensitized solar cell. *Chem. Mater.* **2012**, *24*, 3493–3499.

(21) Hagfeldt, A.; Boschloo, G.; Sun, L.; Kloo, L.; Pettersson, H. Dye-sensitized solar cells. *Chem. Rev.* **2010**, *110*, 6595–6663.

(22) Wang, P.; Zakeeruddin, S. M.; Moser, J. E.; Humphry-Baker, R.; Comte, P.; Aranyos, V.; Hagfeldt, A.; Nazeeruddin, M. K.; Grätzel, M. Stable new sensitizer with improved light harvesting for nanocrystalline dye-sensitized solar cells. *Adv. Mater.* **2004**, *16*, 1806–1811.

(23) Liang, M.; Chen, J. Arylamine organic dyes for dye sensitized solar cells. *Chem. Soc. Rev.* **2013**, *42*, 3453–3488.

(24) Im, H.; Kim, S.; Park, C.; Jang, S. H.; Kim, C. J.; Kim, K.; Park, N. G.; Kim, C. High performance organic photosensitizers for dye-sensitized solar cells. *Chem. Commun.* **2010**, *46*, 1335–1337.

(25) Ning, Z. J.; Tian, H. Triarylamine: A promising core unit for efficient photovoltaic materials. *Chem. Commun.* **2009**, 5483–5495.

(26) Zhou, L.; Jia, C. Y.; Wan, Z.; Li, Z.; Bai, J.; Zhang, L.; Zhang, J.; Yao, X. Triphenylamine-based organic dyes containing benzimidazole derivatives for dye-sensitized solar cells. *Dyes Pigments* **2012**, *95*, 743–750.

(27) Zhang, G. L.; Bala, H.; Cheng, Y. M.; Shi, D.; Lv, X. J.; Yu, Q. J.; Wang, P. High efficiency and stable dye-sensitized solar cells with an organic chromophore featuring a binary π-conjugated spacer. *Chem. Commun.* **2009**, 2198–2200.

(28) Li, G.; Jiang, K. J.; Li, Y. F.; Li, S. L.; Yang, L. M. Efficient structural modification of triphenylamine-based organic dyes for dye-sensitized solar cells. *J. Phys. Chem. C* **2008**, *112*, 11591–11599.

(29) Moon, S. J.; Yum, J. H.; Humphry-Baker, R.; Karlsson, K. M.; Hagberg, D. P.; Marinado, T.; Hagfeldt, A.; Sun, L. C.; Grätzel, M.; Nazeeruddin, M. K. Highly efficient organic sensitizers for solid-state dye-sensitized solar cells. *J. Phys. Chem. C* **2009**, *113*, 16816–16820.

(30) Li, R. Z.; Liu, J. Y.; Cai, N.; Zhang, M.; Wang, P. Synchronously reduced surface states, charge recombination, and light absorption length for high-performance organic dye-sensitized solar cells. *J. Phys. Chem. B* **2010**, *114*, 4461–4464.

(31) Hagberg, D. P.; Jiang, X.; Gabrielsson, E.; Linder, M.; Marinado, T.; Brinck, T.; Hagfeldt, A.; Sun, L. C. Symmetric and unsymmetric donor functionalization: comparing structural and spectral benefits of chromophores for dye-sensitized solar cells. *J. Mater. Chem.* **2009**, *19*, 7232–7238.

(32) Ning, Z. J.; Zhang, Q.; Wu, W. J.; Pei, H. C.; Liu, B.; Tian, H. Starburst triarylamine based dyes for efficient dye-sensitized solar cells. *J. Org. Chem.* **2008**, *73*, 3791–3797.

(33) Tang, J.; Hua, J. L.; Wu, W. J.; Li, J.; Jin, Z. G.; Long, Y. T.; Tian, H. New starburst sensitizer with carbazole antennas for efficient and stable dye-sensitized solar cells. *Energy Environ. Sci.* **2010**, *3*, 1736–1745.

(34) Wan, Z. Q.; Jia, C. Y.; Duan, Y. D.; Zhou, L. L.; Lin, Y.; Shi, Y. Phenothiazine−triphenylamine based organic dyes containing various conjugated linkers for efficient dye-sensitized solar cells. *J. Mater. Chem.* **2012**, *22*, 25140–25147.

(35) Hagberg, D. P.; Edvinsson, T.; Marinado, T.; Boschloo, G.; Hagfeldt, A.; Sun, L. C. A novel organic chromophore for dye-sensitized nanostructured solar cells. *Chem. Commun.* **2006**, 2245–2247.

246

dx.doi.org/10.1021/sc400293v | *ACS Sustainable Chem. Eng.* 2014, 2, 239–247

(36) Li, W. Q.; Wu, Y. Z.; Zhang, Q.; Tian, H.; Zhu, W. H. D-A-π-A Featured sensitizers bearing phthalimide and benzotriazole as auxiliary acceptor: effect on absorption and charge recombination dynamics in dye-sensitized solar cells. *ACS Appl. Mater. Interfaces* **2012**, *4*, 1822.

(37) Sudyoadsuk, T.; Pansay, S.; Morada, S.; Rattanawan, R.; Namuangruk, S.; Kaewin, T.; Jungsuttiwong, S.; Promarak, V. Synthesis and characterization of D−D−π−A-type organic dyes bearing carbazole−carbazole as a donor moiety (D−D) for efficient dye-sensitized solar cells. *Eur. J. Org. Chem.* **2013**, *23*, 5051−5063.

(38) Tian, H.; Yang, X.; Pan, J.; Chen, R.; Liu, M.; Zhang, Q.; Hagfeldt, A.; Sun, L. A triphenylamine dye model for the study of intramolecular energy transfer and charge transfer in dye-sensitized solar cells. *Adv. Funct. Mater.* **2008**, *18*, 3461−3468.

(39) Liu, B.; Liu, Q. B.; You, D.; Li, X. Y.; Naruta, Y.; Zhu, W. H. Molecular engineering of indoline based organic sensitizers for highly efficient dye-sensitized solar cells. *J. Mater. Chem.* **2012**, *22*, 13348−13356.

(40) He, J.; Guo, F.; Li, X.; Wu, W.; Yang, J.; Hua, J. New bithiazole-based sensitizers for efficient and stable dye-sensitized solar cells. *Chem.—Eur. J.* **2012**, *18*, 7903−7915.

(41) Li, R.; Lv, X.; Shi, D.; Zhou, D.; Cheng, Y.; Zhang, G.; Wang, P. Dye-sensitized solar cells based on organic sensitizers with different conjugated linkers: Furan, bifuran, thiophene, bithiophene, selenophene, and biselenophene. *J. Phys. Chem. C* **2009**, *113*, 7469−7479.

(42) Baheti, A.; Thomas, K. R.; Lee, C. P.; Ho, K. C. Fine tuning the performance of DSSCs by variation of the π-spacers in organic dyes that contain a 2,7-diaminofluorene donor. *Chem. Asian J.* **2012**, *7*, 2942−2954.

(43) Frisch, M. J.; Trucks, G. W.; Schlegel, H. B.; Scuseria, G. E.; Robb, M. A.; Cheeseman, J. R.; Scalmani, G.; Barone, V.; Mennucci, B.; Petersson, G. A.; Nakatsuji, H.; Caricato, M.; Li, X.; Hratchian, H. P.; Izmaylov, A. F.; Bloino, J.; Zheng, G.; Sonnenberg, J. L.; Hada, M.; Ehara, M.; Toyota, K.; Fukuda, R.; Hasegawa, J.; Ishida, M.; Nakajima, T.; Honda, Y.; Kitao, O.; Nakai, H.; Vreven, T.; Montgomery, J. A.; Peralta, J. E.; Ogliaro, F.; Bearpark, M.; Heyd, J. J.; Brothers, E.; Kudin, K. N.; Staroverov, V. N.; Kobayashi, R.; Normand, J.; Raghavachari, K.; Rendell, A.; Burant, J. C.; Iyengar, S. S.; Tomasi, J.; Cossi, M.; Rega, N.; Millam, J. M.; Klene, M.; Knox, J. E.; Cross, J. B.; Bakken, V.; Adamo, C.; Jaramillo, J.; Gomperts, R.; Stratmann, R. E.; Yazyev, O.; Austin, A. J.; Cammi, R.; Pomelli, C.; Ochterski, J. W.; Martin, R. L.; Morokuma, K.; Zakrzewski, V. G.; Voth, G. A.; Salvador, P.; Dannenberg, J. J.; Dapprich, S.; Daniels, A. D.; Farkas, O.; Foresman, J. B.; Ortiz, J. V.; Cioslowski, J.; Fox, D. J. *Gaussian 09*, Revision A.02; Gaussian, Inc.: Wallingford CT, 2009.

(44) Becke, A. D. A new mixing of Hartree-Fock and local density-functional theories. *J. Chem. Phys.* **1993**, *98*, 1372−1377.

(45) Yanai, T.; Tew, D. P.; Handy, N. C. A new hybrid exchange−correlation functional using the Coulomb-attenuating method (CAM-B3LYP). *Chem. Phys. Lett.* **2004**, *393*, 51−57.

(46) Ooyama, Y.; Ishii, A.; Kagawa, Y.; Imae, I.; Harima, Y. Dye-sensitized solar cells based on novel donor−acceptor π-conjugated benzofuro[2,3-*c*]oxazolo[4,5-*a*]carbazole-type fluorescent dyes exhibiting solid-state fluorescence. *New J. Chem.* **2007**, *31*, 2076−2082.

(47) Numata, Y.; Islam, A.; Chen, H.; Han, L. Aggregation-free branch-type organic dye with a twisted molecular architecture for dye-sensitized solar cells. *Energy Environ. Sci.* **2012**, *5*, 8548−8552.

(48) Tatay, S.; Haque, S. A.; O'Regan, B.; Durrant, J. R.; Verhees, W. J. H.; Kroon, J. M.; Vidal-Ferran, A.; Gaviña, P.; Palomares, E. Kinetic competition in liquid electrolyte and solid-state cyanine dye sensitized solar cells. *J. Mater. Chem.* **2007**, *17*, 3037−3044.

(49) Pastore, M.; De Angelis, F. Aggregation of organic dyes on TiO$_2$ in dye-sensitized solar cells models: an ab initio investigation. *ACS Nano* **2010**, *4*, 556−562.

(50) Jiang, X.; Marinado, T.; Gabrielsson, E.; Hagberg, D. P.; Sun, L.; Hagfeldt, A. Structural modification of organic dyes for efficient coadsorbent-free dye-sensitized solar cells. *J. Phys. Chem. C* **2010**, *114*, 2799−2805.